ChemComm

COMMUNICATION

View Article Online
View Journal

Cite this: DOI: 10.1039/d6cc01038e

Received 16th February 2026,
Accepted 8th April 2026

DOI: 10.1039/d6cc01038e

rsc.li/chemcomm

Nanoparticle-in-microparticle oral delivery system based on drug-loaded polymeric micelles

Hen Moshe Halamish, Roni Sverdlov Arzi and Alejandro Sosnik *

This work develops and characterises a hierachichal oral drug delivery system based on the microencapsulation of drug-loaded amphiphilic nanogels within a mucoadhesive alginate/chitosan shell. Results show a more controlled release and a statistically significant oral half-life with respect to the free drug.

Low drug solubility in biological fluids leads to limited absorption in the gastrointestinal tract and low oral bioavailability, challenging therapeutic efficacy.[1–3] Over the years, a plethora of delivery systems at different size scales have been engineered to increase aqueous solubility and dissolution rate, physicochemical stability and bioavailability of small-molecule and macromolecular drugs, control their release and target them to body sites, and prolong their circulation time.[4,5] Sustained oral drug delivery is difficult to accomplish due to the short residence time and low permeability across the intestinal epithelium of conventional formulations. Polymeric micelles are nanoparticles generated by the self-assembly of polymeric amphiphiles when the concentration in water is above the critical micellar concentration. Depending on the molecular architecture of the amphiphile, they display a hydrophilic corona and a hydrophobic core or more complex nanostructures[6,7] and they have become a valuable nanotechnology platform for the encapsulation, delivery and targeting of small-molecule lipophilic drugs.[8–10] Recently, more complex self-assembled nanoparticles have been engineered[11] to also fit the encapsulation of biologicals.[12] Historically, these drug nanocarriers have been investigated for intravenous administration though their efficacy in mucosal drug delivery has been proposed.[13–15] We pioneered the use of polymeric micelles in mucosal drug delivery by various administration routes such as oral, intranasal and ocular.[16] Despite the advantages shown by oral polymeric micelles, they usually display burst release, and the harsh gastric conditions could degrade the payload before it undergoes intestinal absorption.[17] To prolong the residence time of nano-drug delivery systems in the gastrointestinal tract, we developed nanoparticle-in-microparticle oral delivery systems (NiMODSs) in which pure drug nanoparticles are microencapsulated within a mucoadhesive matrix.[18,19] The pharmacokinetic (PK) parameter used to estimate bioavailability is the area-under-the-curve (AUC) which correlates with therapeutic efficacy, the greater the AUC, the higher bioavailability and the efficacy.[20] Often, when higher oral bioavailability is achieved, an increase of the maximum plasmatic concentration (C_{max}) is observed. However, a sharp C_{max} increase represents a ''double-edge knife'' because it is directly associated with toxicity. Ideally, drug delivery systems should combine a significant increase the AUC with a low to moderate increase of the C_{max}. Poor oral bioavailability may also increase the variability in the dose–response relationship. NiMODSs exhibit advantageous pharmacokinetic profiles when compared to the free unprocessed and nanonized drugs as they are characterized by a sharp increase of the AUC and a more moderate increase of the C_{max}.[18,19] In addition, they result in longer drug half-life ($t_{1/2}$) which may reduce dosing frequency and patient compliance and smaller variability. Aiming to extend the application of this concept and demonstrate its versatility and modularity, in this work, we investigated a NiMODS comprised of amphiphilic nanogels of a poly(vinyl alcohol)–poly(methyl methacrylate) (PVA-*g*-PMMA) graft copolymer (17% w/w PMMA content) loaded with the tyrosine kinase inhibitor dasatinib (10% w/w payload) and non-covalently crosslinked with boric acid,[21,22] and subsequently encapsulated within alginate matrix microparticles ionotropically crosslinked with calcium cations and chitosan. The use of drug-loaded nanogels instead of pure drug nanoparticles[18,19] expands the ability to control the drug release kinetics. The drug-loaded nanogels were produced by a one-step process in a Y-shape microfluidics device. The hydrodynamic diameter of freshly prepared dasatinib-loaded nanogels, as measured by dynamic light scattering (DLS), was 149 ± 15 and 63 ± 3 nm by intensity and number, respectively, and the polydispersity index 0.296 ± 0.054.[19] To encapsulate them within the mucoadhesive microparticles, they were spray-dried

Laboratory of Pharmaceutical Nanomaterials Science, Faculty of Materials Science and Engineering, Technion-Israel Institute of Technology, Haifa, Israel.
E-mail: chen.moshe.num1@gmail.com, mail2roni@gmail.com, sosnik@technion.ac.il

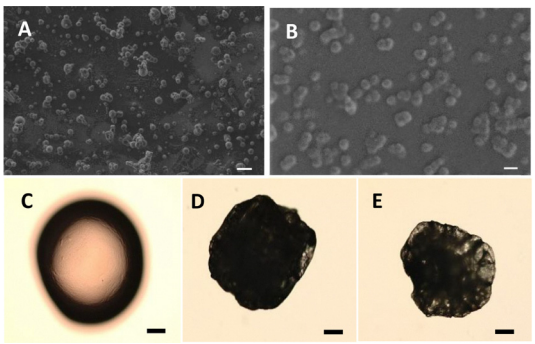

Fig. 1 High Resolution-Scanning electron microscopy micrograph of dasatinib-loaded nanogels (A) after spray-drying in the Büchi Nano Spray Dryer B-90 HP and (B) and re-dispersion in water and casting. (C)–(E) Optical microscopy micrographs of dasatinib-loaded NiMODS produced in the Büchi Encapsulator B-390. (C) Without film-coating, (D) After one film-coating and (E) after two film-coatings. Scale bars: (A) 1 μm, (B) 100 nm and (C)–(E) 10 μm. The drug loading is 1.1% w/w based on dry weight.

utilizing the Büchi Nano Spray Dryer B-90 HP[23] and the dry powder (Fig. 1A) was redispersed in a sodium alginate solution immediately before the microencapsulation stage using the Büchi Encapsulator B-390.[19] The hydrodynamic diameter of spray-dried dasatinib-loaded nanogels upon redispersion in the original volume of water was 129 ± 4 and 54 ± 4 nm by intensity and number, respectively, with a PDI of 0.312 ± 0.004, confirming their very good re-dispersibility. A decrease in the nanogel size upon spray-drying and redispersion is associated with the consolidation of the crosslinked PVA network upon drying. Finally, a two-stage film-coating of the NiMODS with poly(methacrylate) copolymers conferred gastro-resistance and more selective drug release under the gut conditions. The first film-coating stage comprised Eudragit® RL PO, a water-insoluble copolymer of ethyl acrylate, methyl methacrylate, and a low content of methacrylic acid ester with quaternary ammonium groups that swells becoming water-permeable and designed for sustained drug release. The second film-coating was conducted with Eudragit® S100, a copolymer of methacrylic acid and methyl methacrylate in a 1 : 2 weight ratio that is insoluble under acidic pH and dissolves at intestinal pH.[24] The rationale for the double film-coating relies on the selective solubility of the outer film in the gut, exposing the inner one that is water-insoluble and permeable and controls the drug release. The uncoated swollen drug-loaded NiMODS were spherical, with smooth surface and a size of ~1.5 μm (Fig. 1A).

After one and two film-coating cycles, they swelled less and partly lost their spherical shape and surface smoothness (Fig. 1B and C). Their diameter, as measured by optical microscopy, was approximately 30–50 μm, with a final dasatinib loading of 1.1% based on dry weight. NiMODS are envisioned for oral drug delivery. Thus, two polysaccharides with excellent biocompatibility, namely alginate and chitosan, and classified as ''Generally Recognized As Safe'' by the US-Food and Drug Administration were used to produce the microparticles.[25,26] However, drug-loaded PVA-*g*-PMMA nanogels could be released in the gut upon disintegration of the microparticulate matrix.

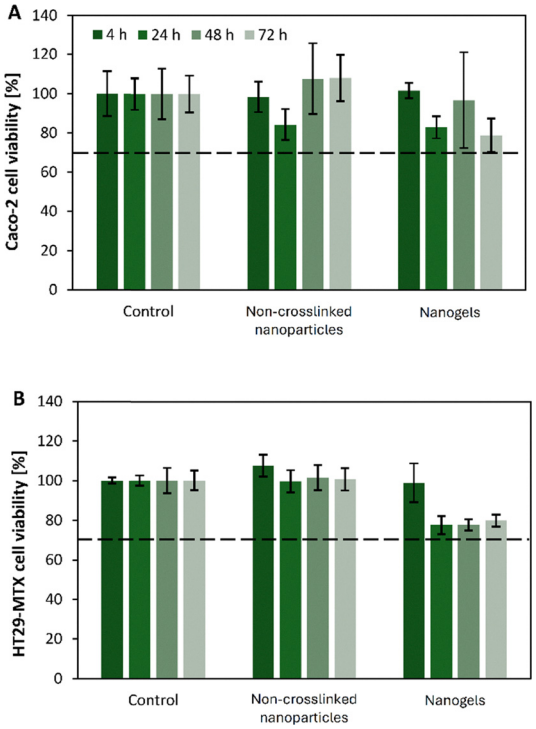

Fig. 2 Viability of (A) Caco-2 and (B) HT29-MTX cells after exposure to dasatinib-free non-crosslinked PVA-*g*-PMMA nanoparticles and nanogels for 4, 24, 48 and 72 h at 37 °C, as determined by the 3-(4,5-dimethylthiazolyl-2)-2,5-diphenyltetrazolium bromide (MTT) assay (n = 3). The dotted line indicates the 70% cell viability acceptable according to the ISO-10993 guidelines.

The compatibility of the nanogels and their non-crosslinked counterparts was assessed in the Caco-2 and HT29-MTX cell lines for 4–72 h. The former is a human colon carcinoma cells line with an enterocyte-like phenotype, while the latter is a mucin-secreting Goblet cell-like line. These cell lines are a reliable model of the intestinal epithelium *in vitro*.[27] Regardless of the incubation time, cell viability was >78% for both types of nanoparticles, indicating that all the nanogel components including boric acid are cell compatible (Fig. 2). These results were with good agreement with previous cell compatibility assays *in vitro*[22,28] and above the value established by the ISO 10993-5 as limit for cell toxicity *in vitro*.[29] The apparent permeability (P_{app}) of the 0.1% w/v non-loaded nanogels was evaluated in a model of the intestinal epithelium *in vitro* based on the co-culture of Caco-2 and HT29-MTX cell lines in a 9 : 1 cell number ratio.[30] The P_{app} was 32.6 ± 3.2 × 10^{-7} cm s^{-1}, in good agreement with previous permeability studies *in vitro* with other amphiphilic nanoparticles of similar size.[31]

The release kinetics of dasatinib from the nanogels and the film-coated NiMODS was assessed *in vitro* using the dialysis membrane method under two different pH conditions that mimic the stomach (pH 1.2) and the small intestine (pH 6.8) and compared to that of the free drug. It is worth noting that the 'release' of the free drug dispersed as solid particles in the same medium of the nanogels comprises the dissolution and permeability of the soluble drug across the dialysis membrane. The outer film-coating of the microparticles withstands the

gastric pH and undergoes dissolution exclusively at the intestinal one, while the inner film-coating is insoluble though permeable to water.[24] In this framework, microparticles slightly swelled though did not disintegrate during the release experiments.[19] Usually, the gastric and small intestine transit time of rats in fasted state is 1–2 h and 3–4 h, respectively.[32] For free drug and nanogels, we conducted the release studies for 4 h because their gastrointestinal transit was not expected to be longer than this. For NiMODSs, we expected to prolong their residence time in the small intestine owing to mucoadhesiveness, and we assessed them for 6 h. At both pH conditions, the release of the nanoencapsulated drug from PVA-*g*-PMMA nanogels was slower than that of the free drug (Fig. S1); a statistically significant difference was measured only after 4 h for pH 1.2 ($p < 0.01$) and after 30 min for pH 6.8 ($p < 0.05$). For example, after 4 h at pH 1.2, the cumulative release of the free drug was 66% compared to 42% of the loaded nanogels (Fig. S1). This indicates that these nanocarriers slow down the release kinetics especially at the beginning of the experiment.[33] Regardless of the strong effect of the pH on the aqueous solubility of dasatinib,[34,35] the release rate of the same formulation in media did not substantially change (Fig. S1). Then, we assessed the dasatinib release from double film-coated NiMODS. At pH 1.2, the outer film does not dissolve which prevents microparticle swelling and cargo release almost completely.[19] Thus, the release from the NiMODS was not assessed under gastric-like conditions. At pH 6.8, the outer coating dissolves, exposing the inner one that is water insoluble though permeable and enables the diffusion of the encapsulated cargo.[19] Microencapsulation within film-coated microparticles resulted in a more sustained release rate with respect to the free drug and the drug-loaded nanogels at pH 6.8 (Fig. 3); 16% of the cargo was released after 4 ($p < 0.01$).

The drug release data were fitted to different release models using the DDSolver add-in program in Microsoft Excel,[36] the Weibull model being the best fit to describe cumulative drug release in solution from matrix-type drug delivery systems.[37] These results suggest that upon oral administration and during the gastrointestinal transit, a more sustained drug release could be achieved. The oral pharmacokinetics of the different formulations was assessed in Sprague-Dawley rats ($n = 6$) and

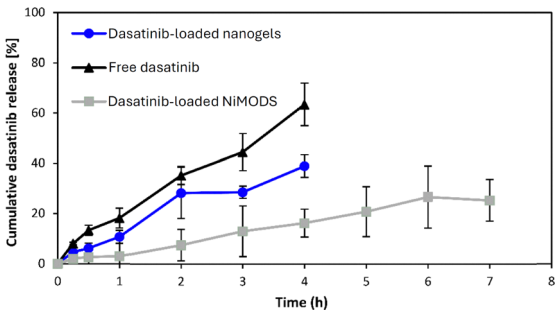

Fig. 3 Dasatinib release *in vitro*, at pH 6.8, under sink conditions. NiMODSs are double film-coated with poly(methacrylate) copolymers. The outer film-coating undergoes dissolution exclusively at intestinal pH, while the inner one is water-insoluble and permeable, remaining intact during the experiment.

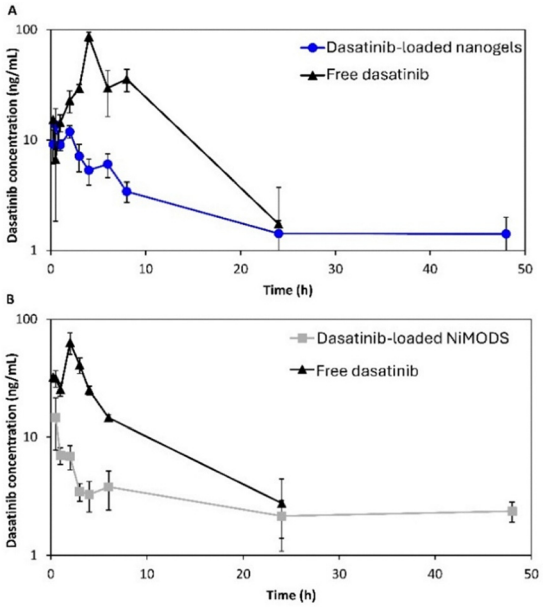

Fig. 4 Mean plasma concentration *versus* time profiles following the oral administration of one single dasatinib dose of (A) 10 mg kg^{-1} and (B) 5 mg kg^{-1}. Formulations were encapsulated within gelatin capsules that disintegrated in the rat mouth ($n = 6$).

data analysed with PKSolver add-in program.[38] We assessed the performance of unprocessed dasatinib and dasatinib-loaded nanogels at a single dose of 10 mg kg^{-1} and of unprocessed dasatinib and double film-coated NiMODSs at a single dose of 5 mg kg^{-1}. Administering a dose of 10 mg kg^{-1} with dasatinib-loaded NiMODSs was not possible in this small animal model due to the relatively low dasatinib loading of this formulation (1.1% w/w) (Fig. 4). For a 10 mg kg^{-1} dose, unprocessed dasatinib showed a C_{max} of 86.4 ng mL^{-1}, a time to the C_{max} (t_{max}) of 3.8 h, an $AUC_{0-\infty}$ of 604.2 ng mL^{-1} h^{-1} and a $t_{1/2}$ of 3.8 h (Fig. 4, Table S1). In this case, dasatinib could not be quantified in plasma after 24 h. For the same dose, dasatinib-loaded nanogels showed a C_{max} of 13.8 ng mL^{-1} that was reached 0.5 h post-administration (as opposed to the 4 h showed by the free drug) and the $AUC_{0-\infty}$ decreased to 168.9 μg mL^{-1} h^{-1}, all the differences between the samples being statistically significant ($p < 0.01$). In addition, the $t_{1/2}$ increased from 3.8 to 19.4 h (Table S1).

These results strongly suggested that the release of dasatinib from the nanogels takes places at a substantially slower rate than the dissolution of free dasatinib (in line with the release results *in vitro*, Fig. 3), leading to a more moderate and prolonged plasma concentration profile. The intrinsic aqueous solubility of dasatinib is a pH-dependent, dramatically increasing at pH <4;[34,35] *e.g.*, 18.4 mg mL^{-1} at pH 2.6 to 0.008 mg mL^{-1} at pH 6.0.[40,41] This could explain the ability of the nanogels to moderate its absorption and reduce its C_{max} with respect to the free drug (Fig. 4A). A decrease of the C_{max} could be associated with lower off-target toxicity, though the sharp decline in the $AUC_{0-\infty}$ may jeopardize therapeutic efficacy of the loaded nanogels.[39] It is important to point out that dasatinib could be absorbed

Table 1 Pharmacokinetic parameters after the oral administration of a single 5 mg kg^{-1} dose of unprocessed dasatinib and double film-coated NiMODSs to Sprague-Dawley rats (n = 6)

	Raw dasatinib		NiMODs	
Pharmacokinetic parameter	Mean	CV %	Mean	CV %
C_{max} (ng mL^{-1})	63.3	30.4	14.6	73.9
$AUC_{0-\infty}$ (μg mL^{-1} h^{-1})	370.0	24.4	366.3	36.1
t_{max} (h)	2.0	47.1	0.5	61.2
$t_{1/2}$ (h)	6.7	63.8	67.2	46.1

better in the stomach due to his strong pH-dependent aqueous solubility.[40,41] Then, we compared the performance of NiMODSs with the free drug upon administration of an oral dose of 5 mg kg^{-1}. Owing to the relatively low dasatinib content of the NiMODSs (1.1%) a 10 mg kg^{-1} dose was unfeasible in rats. As anticipated, double film-coated NiMODSs showed a statistically significant decrease of C_{max} from 63.3 to 14.6 ng mL^{-1} and a dramatic prolongation of the $t_{1/2}$ from 6.7 h to 67.2 h ($p < 0.05$), suggesting that the microparticles undergo mucoadhesion and control the release kinetics in the gastrointestinal tract (Table 1). Furthermore, as opposed to the nanogels, for this dose, the $AUC_{0-\infty}$ of both formulations was almost identical (370.0 and 366.3 μg mL^{-1} h^{-1} for the free and the encapsulated drug, respectively) and statistically insignificant ($p > 0.8$), as shown in Table 1.

Remarkably, a 5-mg kg^{-1} dose with NiMODSs resulted in a 2.2-fold increase of the $AUC_{0-\infty}$ with respect to a 10-mg kg^{-1} dose with nanogels which strongly suggests the key role played by the mucoadhesive microparticles to ensure a more prolonged residence time of the nanogels in the gut and a more efficient release and absorption with respect to the free drug-loaded nanogels. On one hand, the oral bioavailability, as estimated by the $AUC_{0-\infty}$, was substantially lower with the loaded nanogels than with free pure dasatinib nanoparticles.[42] On the other, the C_{max} was more moderate when encapsulated within the microparticles with a similar oral bioavailability which may contribute to lower systemic toxicity.[43] These striking findings highlight the advantage integrating the features of both nanoparticles and microparticles in these hierarchical drug delivery systems to improve the oral bioavailability of poorly water-soluble drugs whereas reducing the impact of the nanoparticulate component on the C_{max} and they pave the way to achieve a better control of the release kinetics and to enhance the bioavailability and therapeutic efficacy of a broad spectrum of orally administered small-molecule and biological drugs.[44–47]

Hen Moshe Halamish: methodology, investigation, data curation, visualization, validation. Roni Sverdlov Arzi: methodology, data curation. Alejandro Sosnik: original draft, visualization, validation, supervision, resources, project administration, methodology, investigation, funding acquisition, conceptualization.

Conflicts of interest

There are no conflicts to declare.

Data availability

Supporting data are included in the supplementary information (SI). Supplementary information: includes the experimental description, the release kinetics of free dasatinib and dasatinib-loaded nanogels *in vitro*, at pH 1.2 and 6.8, and the pharmacokinetic parameters after the oral administration of a single 10 mg kg^{-1} dose of unprocessed dasatinib and dasatinib-loaded nanogels to Sprague-Dawley rats. See DOI: https://doi.org/10.1039/d6cc01038e.

Acknowledgements

The authors would like to thank the financial support of the Uzi & Michal Halevy Fund for Innovative Applied Engineering Research for funding the *in vivo* studies conducted in this work. A.S. thanks the support of the Tamara and Harry Handelsman Academic Chair.

References

1 S. Stegemann, F. Leveiller, D. Franchi, H. de Jong and H. Linden, *Eur. J. Pharm. Sci.*, 2007, **31**, 249–261.
2 P. Li and L. Zhao, *Int. J. Pharm.*, 2007, **341**, 1–19.
3 A. H. Shojaei, *J. Pharm. Pharm. Sci.*, 1998, **1**, 15–30.
4 H. Park, A. Otte and K. Park, *J. Controlled Release*, 2021, **342**, 53–65.
5 P. Wen, W. Ke, A. Dirisala, K. Toh, M. Tanaka and J. Li, *Adv. Drug Delivery Rev.*, 2023, **198**, 114895.
6 V. P. Torchilin, *Adv. Drug Delivery Rev.*, 2002, **54**, 235–252.
7 L. I. Atanase, J. Desbrieres and G. Riess, *Prog. Polym. Sci.*, 2017, **73**, 32–60.
8 H. Cabral, K. Miyata, K. Osada and K. Kataoka, *Chem. Rev.*, 2018, **118**, 6844–6892.
9 M. Ghezzi, S. Pescina, C. Padula, P. Santi, E. Del Favero, L. Cantù and S. Nicoli, *J. Controlled Release*, 2021, **332**, 312–336.
10 W. Jin, Z. Chen, S. Yang, Y. Qu, Y. Pei and Z. Pei, *Chem. Commun.*, 2022, **58**, 12584–12587.
11 M. Panagi, F. Mpekris, P. Chen, C. Voutouri, Y. Nakagawa, J. D. Martin, T. Hiroi, H. Hashimoto, P. Demetriou, C. Pierides, R. Samuel, A. Stylianou, C. Michael, S. Fukushima, P. Georgiou, P. Papageorgis, P. Ch Papaphilippou, L. Koumas, P. Costeas, G. Ishii, M. Kojima, K. Kataoka, H. Cabral and T. Stylianopoulos, *Nat. Commun.*, 2022, **13**, 7165.
12 Q. Shi, H. Yin, R. Song, J. Xu, J. Tan, X. Zhou, J. Cen, Z. Deng, H. Tong, C. Cui, Y. Zhang, X. Li, Z. Zhang and S. Liu, *Nat. Chem.*, 2023, **15**, 257–270.
13 L. Bromberg, *J. Controlled Release*, 2008, **128**, 99–112.
14 G. Gaucher, P. Satturwar, M.-C. Jones, A. Furtos and J.-C. Leroux, *Eur. J. Pharm. Biopharm.*, 2010, **76**, 147–158.
15 S. K. Jena and A. T. Sangamwar, *Carbohydr. Polym.*, 2016, **151**, 1162–1174.
16 A. Sosnik and M. Menaker Raskin, *Biotechnol. Adv.*, 2015, **33**, 1380–1392.
17 H. Al-Lawati and Z. Binkhathlan, *Int. J. Pharm.*, 2025, **687**, 126373.
18 J. C. Imperiale, P. Nejamkin, M. J. Del Sole, C. Lanusse and A. Sosnik, *Biomaterials*, 2015, **37**, 383–394.
19 R. Augustine, D. Levin Ashkenazi, R. Sverdlov Arzi, V. Zlobin, R. Shofti and A. Sosnik, *Acta Biomater.*, 2018, **74**, 344–356.
20 M. Stielow, A. Witczyńska, N. Kubryń, Ł. Fijałkowski, J. Nowaczyk and A. Nowaczyk, *Molecules*, 2023, **28**, 8038.
21 H. Moshe Halamish, J. Trousil, D. Rak, K. D. Knudsen, E. Pavlova, B. Nyström, P. Štěpánek and A. Sosnik, *J. Colloid Interface Sci.*, 2019, **553**, 512–523.
22 H. Moshe Halamish, I. Zlotver and A. Sosnik, *J. Colloid Interface Sci.*, 2022, **626**, 916–929.
23 A. Sosnik and K. P. Seremeta, *Adv. Colloid Interface Sci.*, 2015, **223**, 40–54.
24 A. Nikam, P. R. Sahoo, S. Musale, R. R. Pagar, A. C. Paiva-Santos and P. S. Giram, *Pharmaceutics*, 2023, **15**, 587.
25 M. G. Kontominas, *Foods*, 2020, **9**, 1440.

26 G. Yuan, X. Chen and D. Li, *Food Res. Int.*, 2016, **89**, 117–128.
27 E. Walter, S. Janich, B. J. Roessler, J. M. Hilfinger and G. L. Amidon, *J. Pharm. Sci.*, 1996, **85**, 1070–1076.
28 H. Moshe, Y. Davizon, M. Menaker Raskin and A. Sosnik, *Biomater. Sci.*, 2017, **5**, 2295–2309.
29 International Organization for Standardization (ISO). *ISO 10993-5, Biological Evaluation of Medical Devices, Part 5: Tests for In Vitro Cytotoxicity*, 3rd edn, ISO, Geneva, Switzerland, 2009.
30 P. V. Balimane, S. Chong and R. A. Morrison, *J. Pharmacol. Toxicol. Methods*, 2000, **44**, 301–312.
31 N. Jung, J. Schreiner, F. Baur, S. Vogel-Kindgen and M. Windbergs, *Biomater. Sci.*, 2024, **12**, 5775–5788.
32 C. Tuleu, C. Andrieux, P. Boy and J. C. Chaumeil, *Int. J. Pharm.*, 1999, **180**, 123–131.
33 S. K. R. Adena, M. Upadhyay, H. Vardhan and B. Mishra, *Drug Dev. Ind. Pharm.*, 2018, **44**, 493–501.
34 T. Eley, F. R. Luo, S. Agrawal, A. Sanil, J. Manning, T. Li and A. Blakwood-Chirchir, *J. Clin. Pharmacol.*, 2009, **49**, 700–709.
35 C. Wang, M. Wang, P. Chen, J. Wang and Y. Le, *Pharmaceutics*, 2022, **14**, 197.
36 Y. Zhang, M. Huo, J. Zhou, A. Zou, W. Li, C. Yao and S. Xie, *AAPS J.*, 2010, **12**, 263–271.
37 P. Costa and J. M. Sousa Lobo, *Eur. J. Pharm. Sci.*, 2001, **13**, 123–133.
38 Y. Zhang, M. Huo, J. Zhou and S. Xie, *Comput. Methods Programs Biomed.*, 2010, **99**, 306–314.
39 F. Cheng, Z. Cui, Q. Li, L. Wang, Y. Zhang and W. Li, *Drug Des., Dev. Ther.*, 2025, **19**, 4311–4320.
40 H. J. Šíma, M. Slanař, J. Hořínková, M. Šíma and O. Slanař, *Prague Med. Rep.*, 2019, **120**, 52–63.
41 B. D. Furmanski, S. Hu, K.-I. Fujita, L. Li, A. A. Gibson, L. J. Janke, R. T. Williams, J. D. Schuetz, A. Sparreboom and S. D. Baker, *Clin. Cancer Res.*, 2013, **19**, 4359.
42 R. Sverdlov Arzi, M. Davidovich-Pinhas, N. Cohen and A. Sosnik, *Acta Biomater.*, 2023, **158**, 449–462.
43 F. Cheng, Q. Xu, Q. Li, Z. Cui, W. Li and F. Zeng, *Front. Oncol.*, 2023, **13**, 1113462.
44 Y.-S. Lee, P. J. Johnson, P. T. Robbins and R. H. Bridson, *Eur. J. Pharm. Biopharm.*, 2013, **83**, 168–173.
45 J. Schulze, S. Kuhn, S. Hendrikx, M. Schulz-Siegmund, T. Polte and A. Aigner, *Small*, 2018, **14**, 1701810.
46 Y. Zhang, Y. Wang, Y. Lu, H. Quan, Y. Wang, S. Song and H. Guo, *J. Nanobiotechnol.*, 2025, **23**, 400.
47 P. Xi, X. Wei, Y. Xu, N. Yang, Y. Wang, Y. Huang, M. Chen, Y. Wen, Y. Zhu, Y. Zhao and Z. Gu, *Chem. Eng. J.*, 2024, **498**, 155215.